Granular flows : fluidization and anisotropy

Wortel, G.H.

Chapter 2

Introduction to Flow of Weakly Vibrated Granular Media

A large part of this thesis will be devoted to flow of weakly vibrated granular media. In this chapter we will introduce the subject, describe the setup, and show the *prior results*[1] that were obtained before the work that is reported in chapter 3-5 of this thesis.

2.1 Introduction

In the absence of external forcing, a collection of granular particles jams into a metastable configuration under the influence of gravity-induced pressure and friction. To make the system flow, a shear stress larger than the so-called yield stress has to be imposed, large enough to overcome the friction between the grains. When imposing a stress below the yield stress, the material will not exhibit a steady flow, although typically there will be rearrangements at the micro-scale. For a stress above the yield stress, the material loses its rigidity and will typically start to flow fast. Surprisingly, creating a slow granular flow is not easy or perhaps even possible in a stress-controlled experiment [71].

Flow experiments can also be performed in rate-controlled geometries. In these experiments, slow flows are unstable and the stress appears to be *independent* of the flow rate (for slow enough flows). This is believed to be due to the rate-independence of the microscopic friction law.

[1] J. Dijksman, G. Wortel, L. van Dellen, O. Dauchot, and M. van Hecke, *Jamming, Yielding and Rheology of Weakly Vibrated Granular Media*, Phys. Rev. Lett. **107**, 108303 (2011) [71]

Granular flow in general is induced by imposing either a stress or a strain (rate). In the traditional inclined plane geometry [72, 73], the stress is controlled by changing the tilt angle with respect to gravity. Because of the yield stress, strain-controlled experiments are typically used when studying slow flows [13].

Granular systems can be compared to thermal systems such as glasses [74, 75]. The simple case without external forcing then corresponds to the zero temperature case. Glasses are typically studied in the more interesting case of finite temperature; equivalently, we will study granular materials subject to weak vibrations. We keep the peak acceleration of our vibrations below the gravity acceleration, which means the particles do not fly around as they do in a granular gas, but essentially stay at their relative positions.

During the upward part of the oscillation, gravity is effectively decreased, which makes it easier to make the particles flow. In the experiments, a new, stable, slow, granular flow regime is found where the stress is now *dependent* on the flow rate [13, 71]. This regime, where a granular material can flow slowly under the influence of vibrations, is utilized by many people every morning while gently pouring cereal in a breakfast bowl.

2.2 Setup and Protocol

Split-Bottom Cell – We probe the rheology of weakly vibrated granular flows in a modified split-bottom cell, as shown in Fig. 2.1. The split-bottom cell consists of an acrylic container with an inner radius r_0 of 7.0 cm and a height H of 5.5 cm. The rotating inner disk that drives the flow has a radius r_s of 4 cm and thickness 5 mm. The gap between the container and the disk is about 0.3 mm so no particles can get underneath the disk. To ensure a no-slip boundary condition, the top surface of the disk is made rough by gluing glass particles with diameter of 2 mm to it.

The flow structure in the split-bottom cell depends crucially on the relative filling height H_0/r_s [76]. For low filling heights, the particles above the inner disk corotate with it, whereas the particles close to the outer wall remain stationary. The only location where there is shear between the comoving and the stationary grains, is above the split in the bottom. For higher filling heights, the part of the system that corotates decreases with

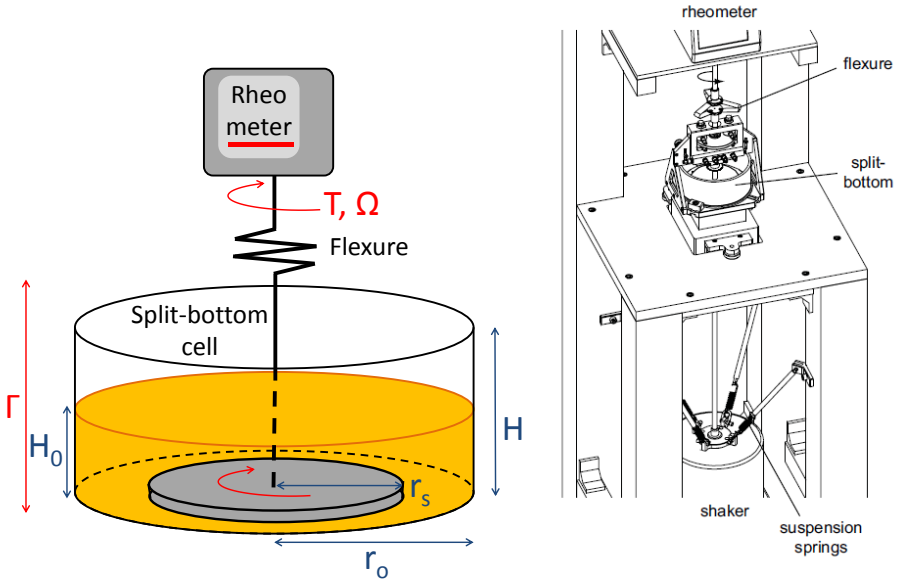

FIGURE 2.1: Left: Sketch of the vibrated split-bottom setup in which the rotation of a disk of radius r_s is used to probe the rheology of agitated granular media. The crucial experimental parameters are the relative filling height, H_0/r_s, vibration strength, Γ, the torque, T, and the rotation rate, Ω. Right: Schematic 3D drawing of the setup including the bearings and the shaker. Figure adapted from [13].

the vertical coordinate z (trumpet flow), and the shear zone widens. Additionally, there is shear between horizontal layers (precession [77]), and the particles at the surface rotate with a lower angular velocity compared to the particles near the bottom. For very high filling heights, the particles at the surface no longer flow, and all the flow is located in a "dome" below the surface.

At slow driving rates, because of symmetry, the experiments can also be performed by rotating the side wall and outer bottom disk, keeping the inner bottom disk stationary.

The split-bottom flow geometry has been studied extensively and produces wide shear zones, and smooth, robust, and well-controlled granular flows [38, 46, 76–85].

Particles and Conditions – The container is filled with particles (black soda-lime glass beads, Sigmund Lindner 4504-007-L), a polydisperse mixture with a diameter between 1 and 1.3 mm, and a bulk density ρ of 1.7×10^3 kg/m^3, up to a filling height H_0. To ensure good reproducibility, we use the total mass of the particles to control H_0. We use black coated beads because those are easier to image than transparent ones.

All experiments are carried out under ambient temperature, pressure, and relative humidity. We have verified that our experiments are insensitive to relative humidities ranging from 6% to 55%. After several months of use, the black coating of the particles visibly deteriorates, and the rheological behavior becomes more sensitive to humidity. We therefore renew our particles on a trimonthly basis, and have found that our experiments reproduce well over the course of several years.

Rheometer – To drive the rotation of the bottom disk and to measure the flow properties of the system, we use a rheometer (Anton Paar DSR 301), which can be used both in stress control (imposing a torque T and measuring the resulting rotation rate Ω) and in rate control (impose Ω, measure T). The native mode of the rheometer is stress control. Therefore, rate-controlled experiments require a feedback loop to adjust the torque such that the desired Ω is reached. The characteristic time of this feedback loop can be altered using the so-called csr-value of the rheometer.

The rheometer can apply a maximum torque of 200 mNm and a maximum rate of 1.66 rps. For comparison, at our maximum filling height, the yield torque is around 33 mNm.

We work with the rheometer using commercial Anton Paar software. This software limits the sample rate to approximately 100 Hz. To acquire data faster, the two analogue output ports are used to read out the torque, rotation rate, or disk deflection angle θ at a time resolution of 15 kHz.

Vibrations – We shake the system with a sinusoidal oscillation $A\sin(2\pi ft)$, with a fixed f of 63 Hz, using an electromagnetic shaker (VTS systems VG100). The amount of vibrations is characterized by the dimensionless parameter $\Gamma = A(2\pi f)^2/g$, where g is the gravitational acceleration. To set Γ, we use a feedback loop built around an accelerometer (Dytran 3120A), and a lock-in amplifier (SRS SR830 DSP), which is executed by software which is developed using LabVIEW. By time-averaging, Γ can be

controlled very accurately with an error in Γ of around 10^{-3} [13].

Coupling – To protect the rheometer against the vibrations, we mount a flexure in the driving axis which is soft (1.4×10^2 N/m) in the vertical direction, but stiff (0.6 Nm/rad) in the rotational direction. The driving axis is fixed with air-bearings (see Fig. 2.1(b)). We avoid using bearings that have mechanical contact with the axis, as that would significantly contribute to the torque. Because the air-bearings can never be perfectly aligned, there is a T-offset of about 25 μNm.

Imaging – We image the surface of the system using a mirror and a Foculus FO114B camera. This allows us to extract the surface flow using particle image velocimetry.

Filling Height – As explained above, in the absence of vibrations, the phenomenology of the flow is determined by the dimensionless filling height $h \equiv H_0/r_s$ [76]. In our experiments, we stay in the low filling height regime ($h \leq 0.6$), where the shear bands are mainly vertical, and all grains above the disk corotate along with it. We have found that in all, but one, flow regimes, the flow profiles observed at the free surface are insensitive to the magnitude of vibrations. For the exception - which is for slow flow and strong vibrations - see Sec. 3.4.3.

Crystallization – In our experiments, there never is crystallization of the particles. The main reason for this is our particle polydispersity. Moreover, even for monodisperse particles, crystallization does not occur at all shaking frequencies and amplitudes [86].

Protocol – In order to obtain reproducible starting conditions, we subject the packing to a preshear before each experiment. The protocol consists of the following amounts of shear: *(i)* 10 s of 1 rps clockwise; *(ii)* 20 s of 1 rps counterclockwise; *(iii)* 10 s of 1 rps clockwise. After this preshear, we wait 10 s before starting the experiment in the clockwise direction. During the preshear and the wait time, the system is already subjected to vibrations. After the wait time, we start the experiment where we either measure $\Omega(T)$ (stress control), or $T(\Omega)$ (rate control).

2.3 Phenomenology

This section describes the previous results that were published in Ref. [71].

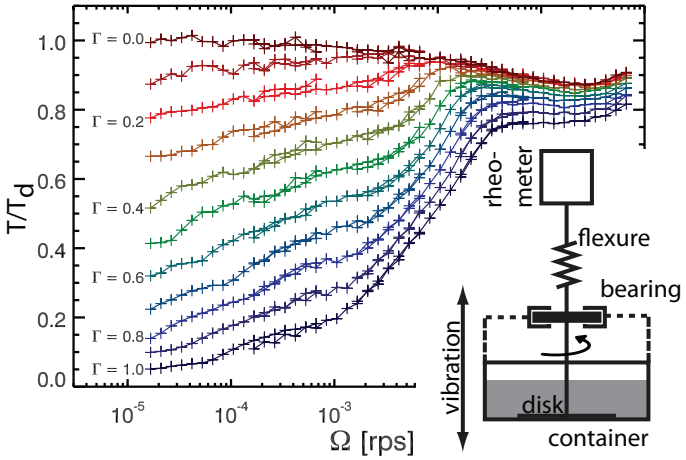

FIGURE 2.2: The flow curves that were measured in rate control for $0 \leq \Gamma \leq 1$ [71]. The T-axis is rescaled with the dynamic yield torque T_d.

2.3.1 $\Gamma = 0$

In Fig. 2.2, we show $T(\Omega)$ flow curves that are measured in rate control for $0 \leq \Gamma \leq 1$ [71], where the torque is rescaled by the dynamic yield torque T_d (here, as in Ref. [71], T_d is defined as the plateau value of T for low Ω and $\Gamma = 0$). On top, there is the flow curve for $\Gamma = 0$. It is not perfectly *rate-independent* but has a *negative slope* that leads to a dip of roughly 10% of the yield torque [87]. The implications of the negative slope are significant: when comparing the situation to pushing a broken car, the negative slope says that if you want the car to go *faster*, you should push *less*. The region of the flow curve that has a negative slope, is the regime that is unstable and unaccessible in torque-controlled experiments [87–89]. For $\Omega \gtrsim 0.1$ rps, the inertial regime is reached and the slope becomes positive [90].

The shape of the $\Gamma = 0$ flow curve qualitatively matches the behavior that is observed when tilting a layer of sand. The sand will make the (hys-

teretic) transition from no flow to fast flow when the static yield stress is reached. If the tilt angle is then decreased again, the sand will keep flowing. Only once the torque corresponding to the dip of the flow curve is reached, the sand stops flowing. If the flow curve would have been perfectly flat, it would have been possible to let sand flow arbitrarily slowly during this decrease of the tilt angle.

We do not exactly know what physically causes the negative slope. It could be related to the rejuvenation of friction, as results similar to this non-monotonic relation between stress and velocity are also found in friction experiments [87, 91, 92]. Alternatively, the negative slope could be the result of shear-induced self-fluidization. In this picture, the system is more fluidized for higher Ω. So, in a certain flow regime, a lower T is required to reach a faster, yet more fluidized, flow. We will discuss this idea in more detail in App. 4.A.3.

2.3.2 $\Gamma > 0$

The flow curves for $\Gamma > 0$ (also plotted in Fig. 2.2) *do* drop to low T for low Ω, suggesting that the yield torque disappears when switching on the vibrations. This is hard to say with certainty for our data range, but we have never observed indications for flattening of the flow curves for low Ω. For $\Gamma \lesssim 0.8$, the curve still has a regime with negative slope. This means that there are now two stable flow regimes, one for slow and one for fast flow. In between, there is an unstable range in Ω. The size of this regime decreases with increasing Γ, and for $\Gamma \gtrsim 0.8$, the flow curves are monotonic.

The curves can also be considered from the point of view of Ω. For fast Ω, T varies little with Γ as the fast inertial flow [93] dominates over the vibrations. The flow at intermediate flow rates is similar to the quasi-static flow regime that was thoroughly studied in the absence of vibrations [77–79, 94]. Besides these known flow regimes [6], the new regime is the one for low Ω, where the vibrations now play a significant role.

2.3.3 Simplest Model

The simplest possible model to describe our system would be to describe the flow behavior in terms of friction where the friction coefficient μ depends on Γ. For $\Gamma = 1$, the friction would vanish, and assuming μ varies

linearly with Γ, the system would yield (or: makes the transition towards fast flow) for $T \sim (1 - \Gamma)$. We see that this simple model does not agree with our data. First, the yield stress seems to disappear completely for any finite $\Gamma < 1$, and we do observe slow but stable flow for $T/T_y + \Gamma < 1$. In addition, the transition to fast flow is significantly above $T/T_y + \Gamma = 1$.

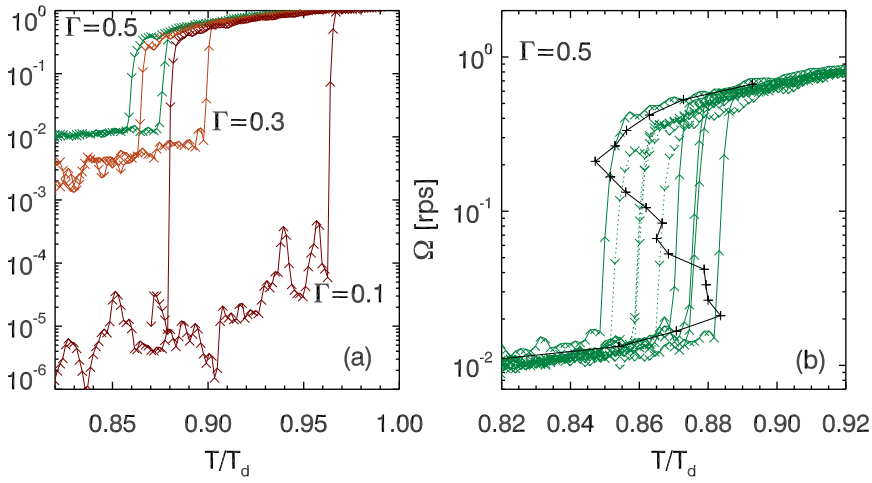

FIGURE 2.3: (a) Finite Γ hysteresis loops for $\Gamma = 0.1, 0.3, 0.5$. (b) Several hysteresis loops for $\Gamma = 0.5$, with the rheological data from $\Gamma = 0.5$ from Fig. 2.2 overplotted in black. Image from [71].

2.3.4 Hysteretic Transition

The next step is to probe whether the negative slope regime of the flow curves for $\Gamma > 0$ leads to hysteresis in torque-controlled experiments [71]. To do so, T/T_d is slowly ramped up and down between 0.8 and 1.1, *i.e.*, through the bistable regime. Fig. 2.3(a) illustrates the resulting hysteresis loops. Ramping upwards, a sudden jump is observed from the slow, mechanically agitated flow branch to the rapid, inertial branch. Ramping back down makes the flow rate jump back to the slow flow branch – there is considerable hysteresis between the stresses where these jumps happen. For smaller Γ, the gap between slow and rapid flow rates increases, con-

sistent with the flow curves shown in Fig. 2.2. In Fig. 2.3(b) the direct connection between the negative slope of the $T(\Omega)$ curve and the hysteresis observed in the $\Omega(T)$ curves is strengthened further for the example of $\Gamma = 0.5$. Several torque-controlled hysteretic data sets are combined with the appropriate flow curve. It can be seen that, while the precise location of individual hysteresis loops fluctuates, the characteristic torques remain confined to an interval which coincides well with the minimum and maximum of the $T(\Omega)$ curve. We conclude that for $\Gamma > 0$, hysteresis and negatively sloped flow curves are directly related.